Flavor dependence of the pion and kaon form factors and parton distribution functions

Parada T. P. Hutauruk,[1] Ian C. Cloët,[2] and Anthony W. Thomas[1]
[1]*CSSM and ARC Centre of Excellence for Particle Physics at the Terascale, Department of Physics, University of Adelaide, Adelaide SA 5005, Australia*
[2]*Physics Division, Argonne National Laboratory, Argonne, Illinois 60439, USA*
(Received 27 April 2016; published 1 September 2016)

The separate quark flavor contributions to the pion and kaon valence quark distribution functions are studied, along with the corresponding electromagnetic form factors in the space-like region. The calculations are made using the solution of the Bethe-Salpeter equation for the model of Nambu and Jona-Lasinio with proper-time regularization. Both the pion and kaon form factors and the valence quark distribution functions reproduce many features of the available empirical data. The larger mass of the strange quark naturally explains the empirical fact that the ratio $u_{K^+}(x)/u_{\pi^+}(x)$ drops below unity at large x, with a value of approximately M_u^2/M_s^2 as $x \to 1$. With regard to the elastic form factors we report a large flavor dependence, with the u-quark contribution to the kaon form factor being an order of magnitude smaller than that of the s-quark at large Q^2, which may be a sensitive measure of confinement effects in QCD. Surprisingly though, the total K^+ and π^+ form factors differ by only 10%. In general we find that flavor breaking effects are typically around 20%.

DOI: 10.1103/PhysRevC.94.035201

I. INTRODUCTION

In our quest to understand the structure of strongly interacting matter, parton distribution functions (PDFs) and electromagnetic form factors are of fundamental importance, and provide complementary information. In an infinite momentum frame picture the former describe the distribution of longitudinal momentum carried by each quark flavor, while the latter are related to their distribution transverse to the beam. There have been numerous studies of hadron PDFs and form factors within quark models of various degrees of sophistication and success, for example, see Refs. [1–17] and [18–32], respectively.

In this paper we focus on the structure of the pion and kaon, with a particular interest in the effects of the larger mass of the strange quark in the kaon. At present, a detailed understanding of pion and kaon structure is hampered by the rather small sample of experimental data [33,34]. The pion PDF has been measured reasonably well in the valence region, and it is known that $u_{K^+}(x)$ is somewhat softer than $u_{\pi^+}(x)$ in the large-x region. While at the present time one does not know the separate flavor contributions to the kaon elastic form factor, it may prove possible to measure them in the future, for example, with a parity violating probe at a future electron ion collider. Further, given the influence of the Drell-Yan-West relation [35,36] and its phenomenological importance, it is of considerable interest to compare the flavor dependence of the large-x PDFs with the corresponding large-Q^2 behavior of the separate flavor contributions to the elastic form factor.

We study the structure of the pion and kaon using the Nambu–Jona-Lasinio (NJL) model with proper-time regularization [37] to simulate the effect of quark confinement [38–40]. The separate contributions of each flavor to the pion and kaon elastic form factors are determined with and without the effect of vector-meson dressing at the quark-photon vertex. In comparison with existing experimental data the model shows excellent agreement. The pion and kaon PDFs are calculated, and the effect of the quark masses on the large-x behavior is explored. We also investigate the effect of the spectator quark mass on the PDF for a given quark flavor, finding satisfactory agreement with the experimental ratio $u_{K^+}(x)/u_{\pi^+}(x)$. We conclude with a discussion of the validity of the Drell-Yan-West relation within this framework.

II. NAMBU–JONA-LASINIO MODEL

The NJL model is a chiral effective theory that mimics many of the key features of quantum chromodynamics (QCD) and is therefore a useful tool to help understand nonperturbative phenomena in low energy QCD [41–45]. For example, the NJL model encapsulates dynamical chiral symmetry breaking (DCSB), which gives rise to dynamically generated dressed quark masses. The NJL model has been successfully used to investigate a broad range of phenomena, including hadron properties [12,46–52], heavy ion collisions [53], neutron stars [45,54,55], quark fragmentation functions [56,57], and transverse momentum dependent phenomena [58].

The three-flavor NJL Lagrangian—containing only four-fermion interactions—takes the form[1]

$$\mathcal{L}_{NJL} = \bar{\psi}(i\partial\!\!\!/ - \hat{m})\psi + G_\pi[(\bar{\psi}\,\lambda_a\,\psi)^2 - (\bar{\psi}\,\lambda_a\,\gamma_5\,\psi)^2] - G_\rho[(\bar{\psi}\,\lambda_a\,\gamma^\mu\,\psi)^2 + (\bar{\psi}\,\lambda_a\,\gamma^\mu\gamma_5\,\psi)^2], \quad (1)$$

where the quark field has the flavor components $\psi = (u,d,s)$, $\hat{m} = \mathrm{diag}(m_u,m_d,m_s)$ denotes the current quark mass matrix, and G_π, G_ρ are four-fermion coupling constants. A sum over $a = 0,\ldots,8$ is implied in Eq. (1), where $\lambda_1,\ldots,\lambda_8$ are the

[1]In principle the two-flavor singlet pieces of the G_ρ term in Eq. (1) can each appear in the NJL interaction Lagrangian with separate coupling constants, as they are individually chirally symmetric. Our choice of identical coupling avoids flavor mixing, giving the flavor content of the ω meson as $u\bar{u} + d\bar{d}$ and the ϕ meson as $s\bar{s}$.

Gell-Mann matrices in flavor space and $\lambda_0 \equiv \sqrt{\frac{2}{3}}\,\mathbb{1}$. The elementary quark-antiquark interaction kernel derived from Eq. (1) takes the form

$$\begin{aligned}\mathcal{K}_{\gamma\delta,\alpha\beta} &= \sum_{\Omega} \mathcal{K}_{\Omega}\,\Omega_{\gamma\delta}\,\bar{\Omega}_{\alpha\beta} \\ &= 2i\,G_\pi[(\lambda_a)_{\gamma\delta}\,(\lambda_a)_{\alpha\beta} + (\lambda_a\,\gamma_5)_{\gamma\delta}\,(\lambda_a\,\gamma_5)_{\alpha\beta}] \\ &\quad - 2i\,G_\rho[(\lambda_a\,\gamma^\mu)_{\gamma\delta}\,(\lambda_a\,\gamma_\mu)_{\alpha\beta} + (\lambda_a\,\gamma^\mu\gamma_5)_{\gamma\delta} \\ &\quad \times (\lambda_a\,\gamma_\mu\gamma_5)_{\alpha\beta}],\end{aligned} \tag{2}$$

where the indices represent Dirac, color, and flavor. In this work we assume that $m_u = m_d = m$, and with the Lagrangian of Eq. (1) the ρ and ω mesons are therefore mass degenerate, differing only in their flavor structure.

The NJL model is non-renormalizable and hence a regularization scheme must be used to control divergences. Here the proper-time scheme is chosen, because it simulates aspects of quark confinement by eliminating on-shell quark propagation, while maintaining the symmetries of the theory, such as the Poincaré and chiral symmetries. As a result it has been widely used [38,39,51,59–64]. Formally the proper-time regularization scheme is defined by

$$\begin{aligned}\frac{1}{X^n} &= \frac{1}{(n-1)!}\int_0^\infty d\tau\,\tau^{n-1}e^{-\tau X} \\ &\longrightarrow \frac{1}{(n-1)!}\int_{1/\Lambda_{\rm UV}^2}^{1/\Lambda_{\rm IR}^2} d\tau\,\tau^{n-1}e^{-\tau X},\end{aligned} \tag{3}$$

where X^n is obtained by first introducing Feynman parametrization and then performing a Wick rotation of the loop momenta to Euclidean space. Only the ultraviolet cutoff, $\Lambda_{\rm UV}$, is needed to render the theory finite. However, in bound states of quarks we also include the infrared cutoff, $\Lambda_{\rm IR}$, which eliminates unphysical thresholds for the decay of hadrons into quarks, therefore implementing quark confinement in the NJL model.

The standard NJL gap equation, illustrated in Fig. 1, provides the dressed quark propagator. The general solution of this gap equation has the form $S_q^{-1}(p) = \not{p} - M_q + i\varepsilon$, where the dressed quark mass for each quark flavour $q = u,d,s$ satisfies

$$M_q = m_q - 4\,G_\pi\,\langle\bar{q}q\rangle = m_q + 12i\,G_\pi\int\frac{d^4k}{(2\pi)^4}\,{\rm Tr}_D[S_q(k)]. \tag{4}$$

The quark condensate is denoted by $\langle\bar{q}q\rangle$ and m_q is the current mass for each quark flavor. Introducing the proper-time

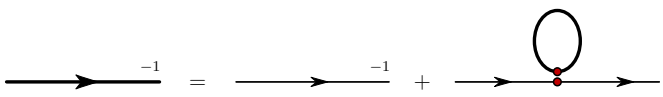

FIG. 1. The NJL gap equation in the Hartree-Fock approximation. The thin line is the bare quark propagator, $S_0^{-1}(k) = \not{k} - m + i\varepsilon$, whereas the thick line is the dressed quark propagator $S(k)$. The $\bar{q}q$ interaction kernel is given by Eq. (2).

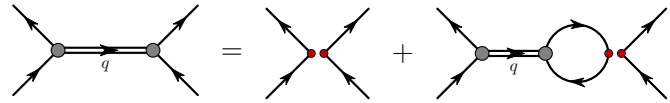

FIG. 2. The BSE in the NJL model, illustrated here for quark and antiquark scattering.

regularization scheme gives

$$M_q = m_q + \frac{3\,M_q\,G_\pi}{\pi^2}\int d\tau\,\frac{1}{\tau^2}\,e^{-\tau\,M_q^2}, \tag{5}$$

where here, and in the following, we drop the proper-time regularization parameters to aid readability. In the chiral limit ($\hat{m} = 0$) the NJL Lagrangian respects the chiral $SU(3)_L \otimes SU(3)_R$ symmetry, however a nontrivial solution ($M_q \neq 0$) to Eq. (4) exists provided $G_\pi > G_{\rm critical}$, which is a signature for DCSB.

The mesons considered here—π, K, ρ, ω, and ϕ—are realized in the NJL model as quark-antiquark bound states whose properties are governed by the Bethe-Saltpeter equation (BSE) illustrated in Fig. 2. This BSE takes the form

$$T(q) = \mathcal{K} + \int\frac{d^4k}{(2\pi)^4}\,\mathcal{K}\,S(k+q)\,T(q)\,S(k), \tag{6}$$

where q is the total four-momentum of the two-body system and the Dirac, color, and flavour indices have been omitted.

The solution to the BSE in the $\alpha = \pi, K$ and $\beta = \rho, \omega, \phi$ channels, are, respectively,[2]

$$T_\alpha(q)_{ab,cd} = [\gamma_5\,\lambda_\alpha]_{ab}\,\tau_\alpha(q)\,[\gamma_5\,\lambda_\alpha^\dagger]_{cd}, \tag{7}$$

$$T_\beta(q)_{ab,cd} = [\gamma_\mu\,\lambda_\beta]_{ab}\,\tau_\beta^{\mu\nu}(q)\,[\gamma_\nu\,\lambda_\beta^\dagger]_{cd}, \tag{8}$$

where λ_α, λ_β are the appropriate flavor matrices, for example, $\lambda_{\pi^0} = \lambda_3$, $\lambda_{\pi^\pm} = \frac{1}{\sqrt{2}}(\lambda_1 \pm i\lambda_2)$, and $\lambda_{K^\pm} = \frac{1}{\sqrt{2}}(\lambda_4 \pm i\lambda_5)$. The reduced t matrices in these channels take the form

$$\tau_\alpha(q) = \frac{-2i\,G_\pi}{1 + 2\,G_\pi\,\Pi_\alpha(q^2)}, \tag{9}$$

$$\tau_\beta^{\mu\nu}(q) = \frac{-2i\,G_\rho}{1 + 2\,G_\rho\,\Pi_\beta(q^2)}\left(g^{\mu\nu} + 2\,G_\rho\,\Pi_\beta(q^2)\,\frac{q^\mu q^\nu}{q^2}\right), \tag{10}$$

and the bubble diagrams appearing read

$$\Pi_\pi(q^2) = 6i\int\frac{d^4k}{(2\pi)^4}{\rm Tr}_D[\gamma_5\,S_\ell(k)\gamma_5\,S_\ell(k+q)], \tag{11}$$

$$\Pi_K(q^2) = 6i\int\frac{d^4k}{(2\pi)^4}\,{\rm Tr}_D[\gamma_5\,S_\ell(k)\gamma_5\,S_s(k+q)], \tag{12}$$

$$\Pi_v^{aa}(q^2)\,P_T^{\mu\nu} = 6i\int\frac{d^4k}{(2\pi)^4}\,{\rm Tr}_D[\gamma^\mu\,S_a(k)\gamma^\nu\,S_a(k+q)], \tag{13}$$

where $\Pi_\rho = \Pi_\omega = \Pi_v^{\ell\ell}$, $\Pi_\phi = \Pi_v^{ss}$, and $\ell \equiv u, d$. The trace is over Dirac indices only and $P_T^{\mu\nu} = g^{\mu\nu} - q^\mu q^\nu/q^2$.

[2]The solution in the pseudoscalar channel can in principle have a pseudovector component ($\not{q}\gamma_5$), however this component is suppressed by m_π/m_{a_1} relative to the leading term and we therefore ignore this contribution.

The meson masses are defined by the pole in the corresponding t matrix, and therefore the pion mass, for example, is determined by the pole condition:

$$1 + 2\,G_\pi\,\Pi_\pi\big(k^2 = m_\pi^2\big) = 0, \tag{14}$$

where analogous results determine m_K, m_ρ, m_ω, and m_ϕ. In fact, because of DCSB the pion and kaon masses are given by the simple expressions

$$m_\pi^2 = \left[\frac{m}{M_\ell}\right]\frac{2}{G_\pi\,\mathcal{I}_{\ell\ell}\big(m_\pi^2\big)}, \tag{15}$$

$$m_K^2 = \left[\frac{m_s}{M_s} + \frac{m}{M_\ell}\right]\frac{1}{G_\pi\,\mathcal{I}_{\ell s}\big(m_K^2\big)} + (M_s - M_\ell)^2, \tag{16}$$

where

$$\mathcal{I}_{ab}(k^2) = \frac{3}{\pi^2}\int_0^1 dx \int \frac{d\tau}{\tau} e^{-\tau[x(x-1)\,k^2 + x\,M_b^2 + (1-x)\,M_a^2]}. \tag{17}$$

This demonstrates the Goldstone boson nature of the pion and kaon in the chiral limit. The residue at a pole in the $\bar{q}q$ t matrices defines the effective meson-quark-quark coupling constant, and for the various mesons we obtain

$$Z_\alpha^{-1} = -\left.\frac{\partial\,\Pi_\alpha(q^2)}{\partial q^2}\right|_{q^2=m_\alpha^2}, \quad \alpha = \pi, K, \rho, \omega, \phi. \tag{18}$$

The parameters of our NJL model are therefore: the couplings in the NJL Lagrangian G_π and G_ρ; the regularization parameters $\Lambda_{\rm IR}$ and $\Lambda_{\rm UV}$; and the u/d and s dressed quark masses (or alternatively their current quark masses). In QCD the confinement scale is set by $\Lambda_{\rm QCD}$ and therefore we fix $\Lambda_{\rm IR} = 240\,$MeV and choose the dressed light quark mass as $M_\ell = 400\,$MeV. The remaining parameters are then fit to the physical pion ($m_\pi = 140\,$MeV), kaon ($m_K = 495\,$MeV), and ρ ($m_\rho = 770\,$MeV) masses, together with the pion decay constant ($f_\pi = 93\,$MeV). This gives $G_\pi = 19.04\,\text{GeV}^{-2}$, $G_\rho = 11.04\,\text{GeV}^{-2}$, $\Lambda_{\rm UV} = 645\,$MeV, and $M_s = 611\,$MeV. Note, for the ϕ mass we obtain $m_\phi = 1001\,$MeV.

Elementary results in this NJL model are presented in Table I. A focus herein is the effect of explicit chiral symmetry and flavor symmetry violation. As a starting point we can consider the Goldberger-Treiman relation at the quark level, and the Gell-Mann–Oakes–Renner relation. For the pion these read

$$f_\pi\sqrt{Z_\pi} = \tfrac{1}{2}(M_u + M_d), \tag{19}$$

$$f_\pi^2\,m_\pi^2 = -\tfrac{1}{2}(m_u + m_d)\langle\bar{u}u + \bar{d}d\rangle, \tag{20}$$

and in the chiral limit these relations are satisfied exactly. With the parameters above we find violation at the 1% level for the pion. However, for the analogous relations for the kaon we find violations at the 20–25 % level, which is sizable, but much less than what may be expected from the current quark mass ratio $2\,m_s/(m_u + m_d) = 27.5 \pm 1.0$ [65,66]. Flavor symmetry breaking effects are therefore consistent with expectations from DCSB and the dressed quark masses: $[M_s - M_\ell]/[M_s + M_\ell] \simeq 21\%$.

TABLE I. Results for the meson-quark-quark coupling constants, kaon leptonic decay constant, and the quark condensates. All dimensioned quantities are in units of GeV.

Z_π	Z_K	Z_ρ	Z_ω	Z_ϕ	f_K	$\langle\bar{u}u\rangle^{1/3}$	$\langle\bar{s}s\rangle^{1/3}$
17.85	20.89	8.44	8.44	13.02	0.097	−0.171	−0.150

III. ELASTIC FORM FACTORS

To determine the electromagnetic current of the pion or kaon we couple the electromagnetic field to the quark fields via minimal substitution: $i\partial\!\!\!/ \to i\partial\!\!\!/ - \hat{Q}\,A_\mu\,\gamma^\mu$, where A_μ is electromagnetic potential, e is the positron charge, and $\hat{Q} = \text{diag}[e_u, e_d, e_s] = \frac{e}{2}(\lambda_3 + \frac{1}{\sqrt{3}}\lambda_8)$ is the quark charge operator, where e_q are the quark charges. The matrix element of the electromagnetic current for a pseudoscalar meson reads

$$J_\alpha^\mu(p', p) = (p'^\mu + p^\mu)F_\alpha(Q^2), \quad \alpha = \pi, K, \tag{21}$$

where p and p' denote the initial and final four momenta of the state, $q^2 = (p' - p)^2 \equiv -Q^2$ and $F_\alpha(Q^2)$ is the pion or kaon form factor.

The pseudoscalar meson form factors in the NJL model are given by the sum of the two Feynman diagrams depicted in Fig. 3, which are respectively given by

$$j_{1,\alpha}^\mu(p', p) = i\,Z_\alpha \int \frac{d^4k}{(2\pi)^4} \times \text{Tr}[\gamma_5\lambda_\alpha^\dagger S(p' + k)\,\hat{Q}\,\gamma^\mu\,S(p + k)\,\gamma_5\,\lambda_\alpha\,S(k)], \tag{22}$$

$$j_{2,\alpha}^\mu(p', p) = i\,Z_\alpha \int \frac{d^4k}{(2\pi)^4} \times \text{Tr}[\gamma_5\lambda_\alpha\,S(k - p)\hat{Q}\,\gamma^\mu\,S(k - p')\,\gamma_5\,\lambda_\alpha^\dagger\,S(k)], \tag{23}$$

where the trace is over Dirac, color, and flavor indices. The index α labels the state and λ_α are the corresponding flavor matrices. In flavor space the quark propagator reads $S(p) = \text{diag}[S_u(p), S_d(p), S_s(p)]$.

We will focus on the quark sector and total form factors for π^+, K^+, and K^0, where for the form factors we find

$$F_{\pi^+}^{(\text{bare})}(Q^2) = (e_u - e_d)f_\pi^{\ell\ell}(Q^2), \tag{24}$$

$$F_{K^+}^{(\text{bare})}(Q^2) = e_u\,f_K^{\ell s}(Q^2) - e_s\,f_K^{s\ell}(Q^2), \tag{25}$$

$$F_{K^0}^{(\text{bare})}(Q^2) = e_d\,f_K^{\ell s}(Q^2) - e_s\,f_K^{s\ell}(Q^2). \tag{26}$$

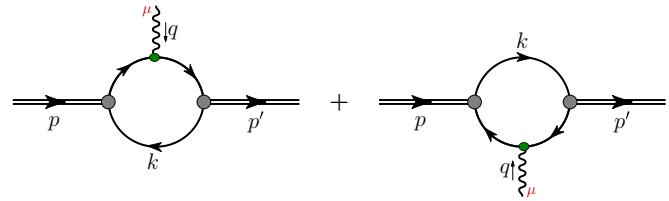

FIG. 3. Diagrammatic representation of the electromagnetic current of the pion or kaon.

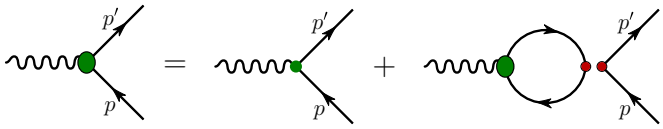

FIG. 4. Illustration of the inhomogeneous BSE which gives the dressed quark-photon vertex. The large shaded oval represents the solution of the inhomogeneous BSE, the small dot is the inhomogeneous driving term ($\hat{Q}\,\gamma^\mu$), and the double-dots represent the $q\bar{q}$ interaction kernel given in Eq. (2).

These results are denoted as "bare" because the quark-photon vertex is the elementary result, that is, $\Lambda^{\mu\,(\mathrm{bare})}_{\gamma q} = \hat{Q}\,\gamma^\mu$. The first superscript on the body form factors, $f^{ab}_\alpha(Q^2)$, indicates the struck quark and the second the spectator, where

$$\begin{aligned} f^{ab}_\alpha(Q^2) = {} & \frac{3\,Z_\alpha}{4\,\pi^2}\int_0^1 dx \int \frac{d\tau}{\tau}\, e^{-\tau[M_a^2+x(1-x)\,Q^2]} \\ & + \frac{3\,Z_\alpha}{4\,\pi^2}\int_0^1 dx \int_0^{1-x} dz \int d\tau \,\big[(x+z)\,m_\alpha^2 \\ & + (M_a - M_b)^2(x+z) + 2\,M_b(M_a - M_b)\big] \\ & \times e^{-\tau[(x+z)(x+z-1)\,m_\alpha^2+(x+z)\,M_a^2+(1-x-z)\,M_b^2+x\,z\,Q^2]}. \end{aligned} \tag{27}$$

Importantly, these expressions satisfy charge conservation exactly.[3]

The quark-sector form factors for a hadron α are defined by

$$F_\alpha(Q^2) = e_u\,F^u_\alpha(Q^2) + e_d\,F^d_\alpha(Q^2) + e_s\,F^s_\alpha(Q^2) + \ldots. \tag{29}$$

Therefore the "bare" pseudoscalar meson quark-sector form factors are easily read from Eqs. (24)–(26).

In general the quark-photon vertex is not elementary ($\hat{Q}\,\gamma^\mu$) but is instead dressed, with this dressing given by the inhomogeneous BSE, which is illustrated in Fig. 4. With the NJL kernel of Eq. (2), the general solution for the dressed quark-photon vertex for a quark of flavor q, has the form

$$\Lambda^\mu_{\gamma\,Q}(p',p) = e_q\gamma^\mu + \left(\gamma^\mu - \frac{q^\mu \not{q}}{q^2}\right) F_Q(Q^2) \to \gamma^\mu F_{1Q}(Q^2), \tag{30}$$

where the final result is used because the $q^\mu \not{q}/q^2$ term cannot contribute to a hadron electromagnetic current because of current conservation. Note, the result after the equality in Eq. (30) clearly satisfies the Ward-Takahashi identity:

$$q_\mu\,\Lambda^\mu_{\gamma\,Q}(p',p) = e_q\big[S_q^{-1}(p') - S_q^{-1}(p)\big]. \tag{31}$$

For the dressed u, d, and s quarks we find

$$F_{1U/D}(Q^2) = e_{u/d}\,\frac{1}{1 + 2\,G_\rho\,\Pi^{\ell\ell}_v(Q^2)}, \tag{32}$$

$$F_{1S}(Q^2) = e_s\,\frac{1}{1 + 2\,G_\rho\,\Pi^{ss}_v(Q^2)}, \tag{33}$$

where the explicit form of the bubble diagram is

$$\Pi^{qq}_v(Q^2) = \frac{3\,Q^2}{\pi^2}\int_0^1 dx \int \frac{d\tau}{\tau}\, x(1-x)\, e^{-\tau[M_q^2+x(1-x)Q^2]}. \tag{34}$$

Therefore, with the NJL Lagrangian of Eq. (1) there is no flavor mixing in the dressed quark form factors, in analogy with the dressed quark masses. The dressed quark form factors are illustrated in Fig. 5. In the limit $Q^2 \to \infty$ these form factors reduce to the elementary quark charges, as expected because of asymptotic freedom in QCD. For small Q^2 these results are similar to expectations from vector meson dominance, where the dressed u and d quarks are dressed by ρ and ω mesons and the dressed s quark by the ϕ meson. Note, the denominators in Eqs. (32) and (33) are the same as the pole condition obtained by solving the BSE in the ρ, ω, or ϕ channels. Therefore, the dressed u and d quark form factors have poles at $Q^2 = -m_\rho^2 = -m_\omega^2$, and the dressed s quark form factor has a pole at $Q^2 = -m_\phi^2$.

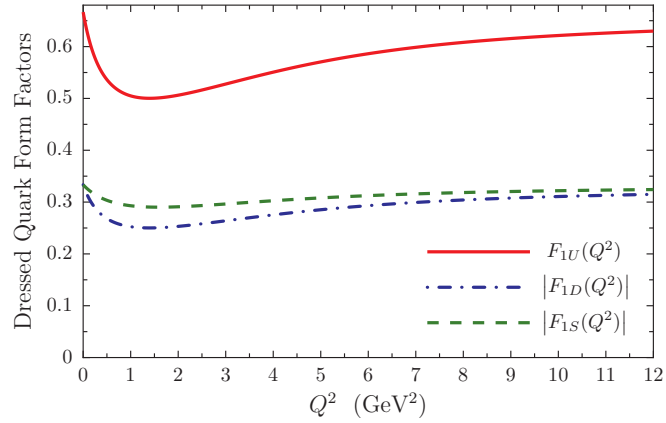

FIG. 5. The dressed quark form factors obtained as solutions to the inhomogeneous BSE.

The complete results for the pseudoscalar meson form factors—with a dressed quark-photon vertex—read

$$F_{\pi^+}(Q^2) = [F_{1U}(Q^2) - F_{1D}(Q^2)]\,f^{\ell\ell}_\pi(Q^2), \tag{35}$$

$$F_{K^+}(Q^2) = F_{1U}(Q^2)\,f^{\ell s}_K(Q^2) - F_{1S}(Q^2)\,f^{s\ell}_K(Q^2), \tag{36}$$

$$F_{K^0}(Q^2) = F_{1D}(Q^2)\,f^{\ell s}_K(Q^2) - F_{1S}(Q^2)\,f^{s\ell}_K(Q^2), \tag{37}$$

where the quark-sector form factors are easily obtained by noting Eq. (29) and the results in Eqs. (32) and (33).

[3]The limit $Q^2 \gg m_\alpha^2$ of the body form factors can be obtained by noting the Feynman parameter domains which dominate the integrals, giving

$$\begin{aligned} Q^2\,f^{ab}_\alpha(Q^2) \overset{Q^2\gg m_\alpha^2}{=} {} & \frac{3\,Z_\alpha}{2\,\pi^2}\int\frac{d\tau}{\tau^2}\,e^{-\tau\,M_a^2} + \frac{3\,Z_\alpha}{2\,\pi^2}\,M_b(M_a - M_b) \\ & \times \int\frac{d\tau}{\tau}\,e^{-\tau\,M_b^2}\big[\gamma_E + \log\big(M_b^2\,\tau\big) + \log\big(Q^2/M_b^2\big)\big]. \end{aligned} \tag{28}$$

Therefore, the form factors receive log corrections at large Q^2 only if $M_a \neq M_b$.

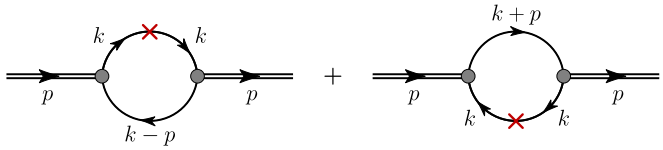

FIG. 6. Feynman diagrams for the valence quark distributions in the pion or kaon. The red cross is the operator insertion $\gamma^+\delta(k^+ - xp^+)\hat{P}_q$, where $\hat{P}_q$ is the projection operator for quarks of flavor q.

IV. VALENCE QUARK DISTRIBUTIONS OF THE KAON

The twist-2 quark distributions in a hadron α are defined by

$$q_\alpha(x) = p^+ \int \frac{d\xi^-}{2\pi}\, e^{ix\,p^+\xi^-}\, \langle \alpha\,|\bar{\psi}_q(0)\gamma^+\psi_q(\xi^-)|\,\alpha\rangle_c, \quad (38)$$

where q is the quark flavor, c denotes a connected matrix element, and $x = \frac{k^+}{p^+}$ is the Bjorken scaling variable, where p^+ is the plus-component of the hadron momentum and k^+ is the plus-component of the struck quark momentum. Note, in the NJL model the gluons are "integrated out" and therefore the gauge-link which should appear in Eq. (38) is unity.

From Eq. (38) one may readily show that the valence quark distribution functions of the pion or kaon are given by the two Feynman diagrams in Fig. 6, where the operator insertion is given by $\gamma^+\delta(k^+ - xp^+)\hat{P}_q$ and $\hat{P}_q$ is the projection operator for quarks of flavor q:

$$\hat{P}_{u/d} = \frac{1}{2}\left(\frac{2}{3}\,\mathbb{1} \pm \lambda_3 + \frac{1}{\sqrt{3}}\,\lambda_8\right), \quad \hat{P}_s = \frac{1}{3}\,\mathbb{1} - \frac{1}{\sqrt{3}}\,\lambda_8. \quad (39)$$

Using the relation $\bar{q}(x) = -q(-x)$ the valence quark and antiquark distributions in the pion or kaon are given by

$$q_\alpha(x) = i\,Z_\alpha \int \frac{d^4k}{(2\pi)^4}\,\delta(k^+ - xp^+) \times \mathrm{Tr}[\gamma_5\lambda_\alpha^\dagger\, S(k)\,\gamma^+\hat{P}_q\, S(k)\,\gamma_5\lambda_\alpha\, S(k-p)], \quad (40)$$

$$\bar{q}_\alpha(x) = -i\,Z_\alpha \int \frac{d^4k}{(2\pi)^4}\,\delta(k^+ + xp^+) \times \mathrm{Tr}[\gamma_5\lambda_\alpha\, S(k)\,\gamma^+\hat{P}_q\, S(k)\,\gamma_5\lambda_\alpha^\dagger\, S(k+p)]. \quad (41)$$

To evaluate these expressions we first take the moments

$$\mathcal{A}_n = \int_0^1 dx\, x^{n-1}\, q(x), \quad (42)$$

where $n = 1, 2, \ldots$ is an integer. Using the Ward-like identity $S(k)\,\gamma^+\,S(k) = -\partial\,S(k)/\partial k_+$ and introducing the Feynman parametrization, the quark and antiquark distributions can then be straightforwardly determined. For the valence quark and antiquark distributions of the K^+ we find

$$q_{K^+}(x) = \frac{3\,Z_K}{4\pi^2}\int d\tau\; e^{-\tau[x(x-1)\,m_K^2 + x\,M_s^2 + (1-x)\,M_\ell^2]} \times \left[\frac{1}{\tau} + x(1-x)\big[m_K^2 - (M_\ell - M_s)^2\big]\right], \quad (43)$$

$$\bar{q}_{K^+}(x) = \frac{3\,Z_K}{4\pi^2}\int d\tau\; e^{-\tau[x(x-1)\,m_K^2 + x\,M_\ell^2 + (1-x)\,M_s^2]} \times \left[\frac{1}{\tau} + x(1-x)\big[m_K^2 - (M_\ell - M_s)^2\big]\right]. \quad (44)$$

Results for the π^+ are obtained by $M_s \to M_\ell$ and $Z_K \to Z_\pi$, giving the result $u_{\pi^+}(x) = \bar{d}_{\pi^+}(x)$. The quark distributions for the other pseudoscalar mesons can be determined using flavor symmetries.

The quark distributions satisfy the baryon number and momentum sum rules, which for the K^+ read

$$\int_0^1 dx[u_{K^+}(x) - \bar{u}_{K^+}(x)] = \int_0^1 dx[\bar{s}_{K^+}(x) - s_{K^+}(x)] = 1, \quad (45)$$

for the number sum rule and at the model scale the momentum sum rule is given by

$$\int_0^1 dx\; x[u_{K^+}(x) + \bar{u}_{K^+}(x) + s_{K^+}(x) + \bar{s}_{K^+}(x)] = 1. \quad (46)$$

Analogous results hold for the remaining kaons and the pions.

V. ELASTIC FORM FACTORS RESULTS

Results for the pion form factor—including effects from the dressed quark-photon vertex—are presented in Figs. 7 and 8, where comparisons to data [67–72], an empirical parametrization [67] and the Dyson-Schwinger equation (DSE) result of Ref. [31] have been made. We find excellent agreement with existing data and the modest differences with

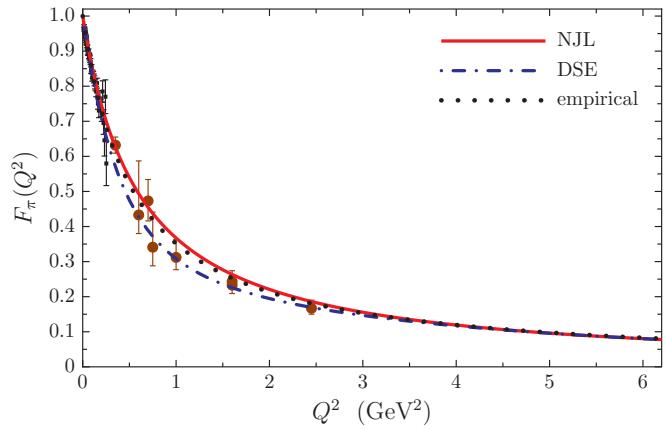

FIG. 7. Our results for the pion form factor are given as the solid line and a comparison is made to the DSE results of Ref. [31]. The empirical result (dotted line) has the form $F_\pi(Q^2) = [1 + Q^2/\Lambda_\pi^2]^{-1}$, where the mass parameter is chosen to reproduce empirical radius found in Ref. [67], giving $\Lambda_\pi^2 = 0.54\,\mathrm{GeV}^2$. The experimental data is from Refs. [67–72].

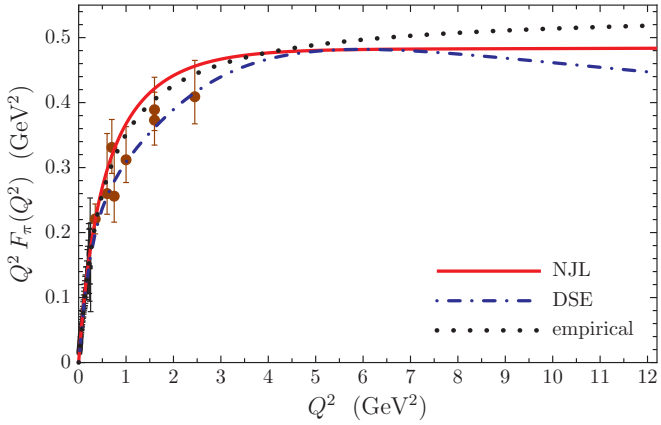

FIG. 8. Results for $Q^2 F_\pi(Q^2)$. See caption to Fig. 7 for the nomenclature.

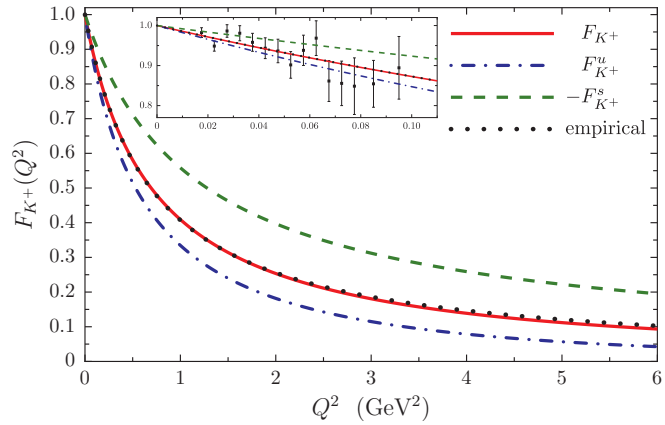

FIG. 9. The K^+ form factor (solid line) together with the up (dashed-dotted line) and strange (dashed line) quark sector contributions. The dotted-line is the fit to data using the form $F_K(Q^2) = [1 + Q^2/\Lambda_K^2]^{-1}$, giving $\Lambda_K^2 = 0.687\,\text{GeV}^2$, and the insert compares our results with existing data taken from Ref. [74].

the DSE result for $Q^2 \lesssim 6\,\text{GeV}^2$ are easily understood. The DSE result drops more rapidly than our NJL result primarily because the Bethe-Salpeter vertices in the DSE approach are non-point-like and thereby suppress large relative momentum between the dressed-quark and dressed-antiquark in the bound state. Our result for $Q^2\,F_\pi(Q^2)$ is very similar to the empirical monopole result but begins to plateau for $Q^2 \gtrsim 6\,\text{GeV}^2$, where $Q^2\,F_\pi(Q^2) \simeq 0.49$. This maximum is almost identical to that obtained using the DSEs, which is not surprising because in both approaches it is driven by DCSB [41,42,73]. This is made clear from Eqs. (5) and (28), which in the chiral limit give

$$Q^2\,F_\pi(Q^2) \overset{Q^2 \gg m_\pi^2}{\simeq} -2\,\frac{M_\ell}{f_\pi^2}\,\langle\bar{\ell}\ell\rangle, \tag{47}$$

where each quantity is an order parameters for DCSB. For $Q^2 \gtrsim 6\,\text{GeV}^2$ the DSE result for $Q^2\,F_\pi(Q^2)$ begins to decrease, which is a consequence of QCD's running coupling and a feature which is absent in our NJL calculations.

Results for the K^+ form factor and the quark-sector components—each including effects from the dressed quark-photon vertex—are given in Figs. 9 and 10. We find excellent agreement with the data from Ref. [74] and the empirical monopole $F_K(Q^2) = [1 + Q^2/\Lambda_K^2]^{-1}$ determined by reproducing the charge radius of Ref. [74]. In contrast to the pion, all existing data for the kaon form factor lies in the domain $0 < Q^2 < 0.1\,\text{GeV}^2$, and therefore we eagerly await any new data at Q^2 similar to the pion [75]. For the quark-sector form factors we observe a very large difference in their Q^2 evolution, with the s quark component much harder than the u quark form factor. When weighted by the charges, as in Fig. 10, we find that the s quark component begins to dominate the K^+ form factor for $Q^2 \geq 1.6\,\text{GeV}^2$, becoming completely dominant at very large Q^2.

Results for the pion and kaon radii are listed in Table II. For the pion we find a radius 6% smaller than the Particle Data Group value [76] and agree within errors for both the K^+ and K^0 radii. We find that r_{K^+} is about 7% smaller than r_{π^+}, which is driven by the quark-sector result $|r^s_{K^+}| < |r^d_{\pi^+}|$, with $r^s_{K^+}/r^d_{\pi^+} = 0.70$. We find the perhaps surprising result that $r^u_{K^+} > r^u_{\pi^+}$, with $r^u_K/r^u_\pi = 1.027$ a measure of environment sensitivity for the u quark. These quark-sector radii are listed in Table II. As a measure of flavour breaking we have $[r_{\pi^+} - r_{K^+}]/[r_{\pi^+} + r_{K^+}] = 0.035$ and $[r^u_{K^+} + r^s_{K^+}]/[r^u_{K^+} - r^s_{K^+}] = 0.19$, which would vanish in the $SU(3)$ flavor limit. We therefore find that in some observables flavour breaking effects may be as large as 20%.

In Fig. 11 we illustrate the ratio $F_{K^+}(Q^2)/F_{\pi^+}(Q^2)$ which is always greater than unity and becomes almost constant for $Q^2 \gtrsim 3\,\text{GeV}^2$. For very large Q^2 this ratio plateaus to the value 1.10, in numerical agreement with the QCD result in the conformal limit [77]:

$$F_{K^+}(Q^2)/F_{\pi^+}(Q^2) \overset{Q^2 \gg \Lambda^2_{\rm QCD}}{\longrightarrow} f_K^2/f_\pi^2, \tag{48}$$

however we find $f_K = 97.3\,\text{MeV}$ whereas the empirical value is $f_K = 110.4 \pm 0.8$ [76]. When expressed in terms of the

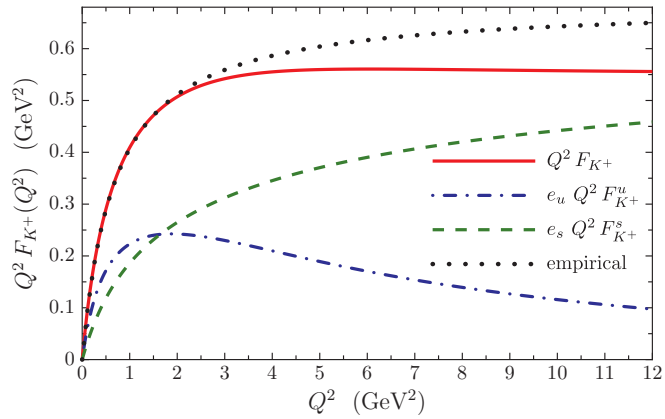

FIG. 10. Results for $Q^2\,F_{K^+}(Q^2)$ together with the charge-weighted quark-sector contributions and the empirical result obtained from Ref. [74]. This result clearly illustrates that the s quark dominates the form factor at large Q^2.

TABLE II. Charge radius results for the pion and kaon, together with the various quark-sector contributions. All radii are in units of fm and the empirical results are from Refs. [65,76].

	r^{expt}	r	r_u	r_d	r_s
π^+	0.672 ± 0.008	0.629	0.629	-0.629	0
K^+	0.560 ± 0.031	0.586	0.646	0	-0.441
K^0	-0.277 ± 0.018	-0.272	0	0.646	-0.441

quark sector form factors, and in the $m_u = m_d$ limit, we have

$$\frac{F_{K^+}(Q^2)}{F_{\pi^+}(Q^2)} = e_u \frac{F^u_{K^+}(Q^2)}{F^u_{\pi^+}(Q^2)} - e_s \frac{F^s_{K^+}(Q^2)}{F^d_{\pi^+}(Q^2)}, \tag{49}$$

where the various quark-sector ratios are also given in Fig. 11. It is clear therefore, that the large constant ratio $F_{K^+}(Q^2)/F_{\pi^+}(Q^2)$ conceals dramatic flavor breaking effects in the quark-sector form factors that grow with increasing Q^2. In the $SU(3)$ flavor limit all ratios in Fig. 11 would be unity for all Q^2. However, at $Q^2 = 10\,\text{GeV}^2$ we find $F^u_{K^+}/F^u_{\pi^+} \simeq 0.36$ and $F^s_{K^+}/F^d_{\pi^+} \simeq 2.74$. Therefore, at large Q^2 we find very large flavor breaking and environment sensitivity effects. The final ratio illustrated in Fig. 11 is $F^u_{K^+}(Q^2)/F^s_{K^+}(Q^2)$, which rapidly drops with increasing Q^2. This behavior can be understood by noting that a form factor is a measure of the ability of a hadron to absorb an electromagnetic current and remain a hadron. In the case of the K^+, if the u quark interacts with the electromagnetic current it must drag along the heavier s quark for the K^+ to remain intact, which becomes increasingly more difficult at larger Q^2 than if the struck quark is an s quark. Therefore this ratio may well be a very sensitive measure of confinement effects in QCD. This behavior is markedly different from what may be expected from a vector meson dominance picture, where $F^u_{K^+}(Q^2)/F^s_{K^+}(Q^2) \simeq [1 + Q^2/m_\phi^2]/[1 + Q^2/m_\rho^2]$, which for $Q^2 \gg 0$ implies $F^u_{K^+}(Q^2)/F^s_{K^+}(Q^2) \to m_\rho^2/m_\phi^2 \simeq 0.56$. However, such a picture is only strictly valid in the neighborhood of the vector meson poles and therefore does not encapsulate environment and confinement effects for large spacelike momenta.

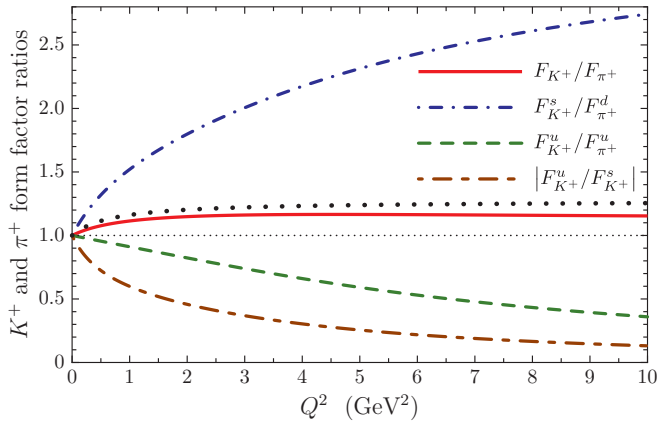

FIG. 11. We illustrate various pion and kaon form factor ratios, including for the quark sector form factors, to ascertain a measure of flavor breaking and environment sensitivity effects as a function of Q^2. Note, all ratios would be unity for all Q^2 in the $SU(3)$ flavor limit.

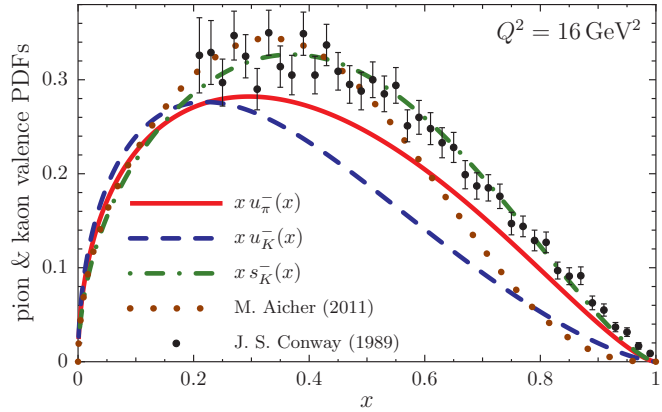

FIG. 12. Results for the valence (minus-type) quark distributions of the π^+ and K^+, evolved from the model scale using the NLO DGLAP equations [78–81]. The solid line represents the valence u or $\bar{d}$ PDF in the π^+, the dot-dashed line is the valence $\bar{s}$ quark, and the dashed line the valence u quark in the K^+. The experimental data is for the π^- and are from Ref. [34]. The dotted line is a reanalysis of this data from Ref. [82].

VI. PARTON DISTRIBUTION FUNCTION RESULTS

Results for the pion and kaon valence PDFs at $Q^2 = 16\,\text{GeV}^2$ are presented in Fig. 12 and compared to empirical data for the pion valence PDF from Ref [34]. The calculated pion valence distribution (solid curve) sits a little below the data. However, a reanalysis of this data was made in Ref. [82] where next-to-leading (NLO) logarithmic threshold resummation effects were included and this result is illustrated as the dotted curve in Fig. 12. The theoretical curve still sits below the new version of the data for x in the region (0.2,0.5) but above it at larger x. Since we do not have a full understanding of the errors on the original or the reanalyzed data, it is difficult to draw firm conclusions but the comparison suggests that the NJL model may not be capturing all of the physics of the pion PDF.

Our results have been evolved using the NLO DGLAP evolution equations [78–81] from a model scale of $Q_0^2 = 0.16\,\text{GeV}^2$, which was independently determined in Ref. [12] in the study of nucleon PDFs. At the model scale we find that the momentum fraction carried by the u and s quarks in the K^+ equal $\langle x\,u\rangle = 0.42$ and $\langle x\,s\rangle = 0.58$ (at this scale gluons carry no momentum so these results saturate the momentum sum rule). We therefore find flavor breaking effects of $[\langle x\,s\rangle - \langle x\,u\rangle]/[\langle x\,s\rangle + \langle x\,u\rangle] \simeq 16\%$ which is similar to that seen in the masses: $[M_s - M_u]/[M_s + M_u] \simeq 21\%$ and quark-sector radii. As another measure of *SU(3)* flavor breaking we note that at the model scale $u_K(x)$ peaks at $x_u = 0.237$ and $\bar{s}_K(x)$ peaks at $x_s = 1 - x_u = 0.763$, which implies flavor breaking effects of around $[x_s - x_u]/[x_s + x_u] \simeq 53\%$. Note that in the *SU(3)* flavor limit these distributions would peak at $x = 0.5$, which is the case for the pion when $m_u = m_d$.

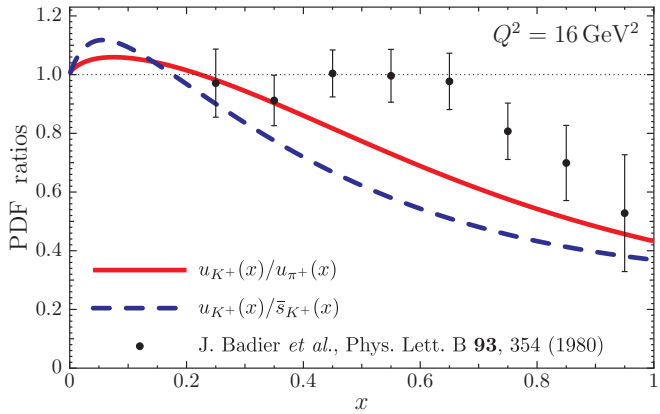

FIG. 13. The solid line gives the ratio of the u quark distribution in the K^+ to the u quark distribution in the π^+, after NLO evolution to $Q^2 = 16\ \mathrm{GeV}^2$. The dashed line gives the ratio of the u quark to $\bar{s}$ quark distributions in the K^+ at $Q^2 = 16\ \mathrm{GeV}^2$. The data are from Ref. [33] and correspond to the ratio $\bar{u}_{K^-}/\bar{u}_{\pi^-}$, which is related to our π^+ and K^+ results by charge symmetry.

The ratio $u_{K^+}(x)/u_{\pi^+}(x)$ is illustrated in Fig. 13 at $Q^2 = 16\,\mathrm{GeV}^2$, however this ratio has only a slight Q^2 dependence and in the limit $x \to 1$ is a fixed point in Q^2. We find $u_{K^+}/u_{\pi^+} \to 0.434 \simeq M_u^2/M_s^2$ as $x \to 1$, in good agreement with existing data from Ref. [83]. However, the x dependence differs from much of the data in the valence region, the reason for this discrepancy is not clear, however it may lie with the absence of momentum dependence in standard NJL Bethe-Salpeter vertices [14,17,84], or with the data itself. We note however the correspondence that $u_{K^+}/u_{\pi^+} < 1$ as $x \to 1$ and that $F_K^u(Q^2)/F_\pi^u(Q^2) < 1$ for $Q^2 \gg \Lambda_{\mathrm{QCD}}^2$. Figure 13 also illustrates the ratio $u_{K^+}(x)/s_{K^+}(x)$, which approaches 0.37 as $x \to 1$. It is evident that flavor breaking effects have a sizable x dependence, being maximal at large x while becoming negligible at small x where perturbative effects from DGLAP evolution dominate.

The limit $x \to 1$ corresponds to elastic scattering from the target and as such it is natural to expect a correspondence between form factors and PDFs in this limit. Such a correspondence was first considered by Drell and Yan [35], and West [36], finding the relation

$$F(Q^2) \overset{Q^2 \gg \Lambda_{\mathrm{QCD}}}{\sim} \frac{1}{Q^{2n}} \quad \Longleftrightarrow \quad q(x) \overset{x \to 1}{\sim} (1-x)^{2n-1}, \quad (50)$$

between a hadron's form factor and PDF, where n is the number of spectators. For the pion the expectation is $F_\pi(Q^2) \overset{Q^2 \gg \Lambda_{\mathrm{QCD}}}{\sim} 1/Q^2$ and therefore the Drell-Yan-West (DYW) relation implies $q_\pi(x) \overset{x \to 1}{\sim} (1-x)$, in good agreement with the data in Fig. 12. For the pion however the DYW relation is in disagreement with the more rigorous QCD analyses of Refs. [77,85], that find

$$F_\pi(Q^2) \overset{Q^2 \gg \Lambda_{\mathrm{QCD}}}{\sim} \frac{1}{Q^2} \quad \Longleftrightarrow \quad q_\pi(x) \overset{x \to 1}{\sim} (1-x)^2, \quad (51)$$

which is consistent with the pion PDF analysis from Ref. [82]. The conclusion argued therefore in Ref. [77] is the the DYW relation is not generally valid in QCD, although it does appear to hold for baryon states. At the model scale our NJL calculation for the pion satisfies

$$F_\pi(Q^2) \overset{Q^2 \gg \Lambda_{\mathrm{QCD}}}{\sim} \frac{1}{Q^2} \quad \Longleftrightarrow \quad q_\pi(x) \overset{x \to 1}{\sim} (1-x)^0, \quad (52)$$

and therefore does not agree with the DYW relation. On the other hand, after DGLAP evolution to $Q^2 \sim 10\,\mathrm{GeV}^2$ the pion and kaon PDFs do behave as $q_\pi(x) \overset{x \to 1}{\sim} (1-x)^1$ as evident in Fig. 12. As a reflection of the expectations of what may be expected by DYW-like relations we find that $u_{K^+}/s_{K^+} < 1$ as $x \to 1$ and $|F_{K^+}^u/F_{K^+}^s| < 1$ for $Q^2 \gg \Lambda_{\mathrm{QCD}}$.

VII. SUMMARY

We have used the NJL model—with proper-time regularization to simulate the effect of confinement—to calculate the electromagnetic form factors and PDFs of the pion and kaon. For the former we included the effect of vertex dressing through vector meson like correlations in the t channel. Particular attention was paid to the individual quark flavor contributions, together with the associated flavor breaking and environment sensitivity effects.

This work produced several interesting results. Firstly, as illustrated in Figs. 9–11, the effect of the larger mass of the strange quark on the electromagnetic form factors is dramatic. Indeed, even though $|e_s| < |e_u|$ the s quark dominates the total elastic form factor of the K^+ for large Q^2. It is argued that these large flavor breaking effects may be a sensitive measure of confinement effects in QCD. Surprisingly however, even though there are very significant changes in the individual flavour contributions in the kaon, the total pion and kaon form factors lie within about 10–15 % for all Q^2, with the environmental suppression of the u quark form factor in the K^+ more or less compensated for by the increase in the strange quark form factor over that of the d quark. This is illustrated in Fig. 11. In terms of the overall agreement with experiment, the total kaon form factor agrees very well with the limited existing data. In the case of the pion, the data extends to much larger Q^2, where again we find excellent agreement.

The effects of the heavier strange quark mass on the PDFs is less spectacular. In Fig. 12 we saw that the strange quark PDF in the K^+ is considerably enhanced over that of the u quark in the valence region. Most importantly, as we see in Fig. 13, the empirical suppression of u_{K^+} compared with u_{π^+} in the large-x region is reproduced. The comparison of the asymptotic behavior of the individual quark-sector form factors and PDFs is fascinating, and the DYW relation was found to hold only after DGLAP evolution of the parton distributions. Numerous other effects of flavor breaking have also been determined, for example, the pion and kaon charge radii, and effects of around 20% were typically observed.

ACKNOWLEDGMENTS

This work was supported by the U.S. Department of Energy, Office of Science, Office of Nuclear Physics, contract no. DE-AC02-06CH11357 and the Australian Research Council through the ARC Centre of Excellence in Particle Physics at the Terascale and an ARC Australian Laureate Fellowship FL0992247 at the University of Adelaide.

[1] E. L. Berger and S. J. Brodsky, Phys. Rev. Lett. **42**, 940 (1979).
[2] A. I. Signal and A. W. Thomas, Phys. Rev. D **40**, 2832 (1989).
[3] T. Shigetani, K. Suzuki, and H. Toki, Phys. Lett. B **308**, 383 (1993).
[4] T. Shigetani, K. Suzuki, and H. Toki, Nucl. Phys. A **579**, 413 (1994).
[5] R. M. Davidson and E. Ruiz Arriola, Phys. Lett. B **348**, 163 (1995).
[6] T. Frederico and G. A. Miller, Phys. Rev. D **50**, 210 (1994).
[7] K. Kusaka, G. Piller, A. W. Thomas, and A. G. Williams, Phys. Rev. D **55**, 5299 (1997).
[8] W. Bentz, T. Hama, T. Matsuki, and K. Yazaki, Nucl. Phys. A **651**, 143 (1999).
[9] H. Weigel, E. Ruiz Arriola, and L. P. Gamberg, Nucl. Phys. B **560**, 383 (1999).
[10] M. B. Hecht, C. D. Roberts, and S. M. Schmidt, Phys. Rev. C **63**, 025213 (2001).
[11] C. Avila, J. C. Sanabria and J. Magnin, Phys. Rev. D **67**, 034022, (2003); **68**, 079902(E) (2003).
[12] I. C. Cloët, W. Bentz, and A. W. Thomas, Phys. Lett. B **621**, 246 (2005).
[13] M. Alberg and J. Tibbals, Phys. Lett. B **709**, 370 (2012).
[14] T. Nguyen, A. Bashir, C. D. Roberts, and P. C. Tandy, Phys. Rev. C **83**, 062201 (2011).
[15] S. I. Nam, Phys. Rev. D **86**, 074005 (2012).
[16] L. Chang and A. W. Thomas, Phys. Lett. B **749**, 547 (2015).
[17] C. Chen, L. Chang, C. D. Roberts, S. Wan, and H. S. Zong, Phys. Rev. D **93**, 074021 (2016).
[18] N. Zovko, Phys. Lett. B **51**, 54 (1974).
[19] H. Ito, W. W. Buck, and F. Gross, Phys. Rev. C **45**, 1918 (1992).
[20] H. J. Schulze, J. Phys. G **20**, 531 (1994).
[21] W. W. Buck, R. A. Williams, and H. Ito, Phys. Lett. B **351**, 24 (1995).
[22] C. D. Roberts, Nucl. Phys. A **605**, 475 (1996).
[23] R. H. Lemmer, Nucl. Phys. A **593**, 315 (1995).
[24] C. J. Burden, C. D. Roberts, and M. J. Thomson, Phys. Lett. B **371**, 163 (1996).
[25] P. C. Tandy, Prog. Part. Nucl. Phys. **39**, 117 (1997).
[26] Z. G. Wang, S. L. Wan, and K. L. Wang, Chin. Phys. **10**, 497 (2001).
[27] J. Bijnens and P. Talavera, J. High Energy Phys. 03 (2002) 046.
[28] O. A. T. Dias, V. S. Filho, and J. P. B. C. de Melo, Nucl. Phys. Proc. Suppl. **199**, 281 (2010).
[29] E. O. da Silva, J. P. B. C. de Melo, B. El-Bennich, and V. S. Filho, Phys. Rev. C **86**, 038202 (2012).
[30] C. Chen, L. Chang, C. D. Roberts, S. M. Schmidt, S. Wan, and D. J. Wilson, Phys. Rev. C **87**, 045207 (2013).
[31] L. Chang, I. C. Cloët, C. D. Roberts, S. M. Schmidt, and P. C. Tandy, Phys. Rev. Lett. **111**, 141802 (2013).
[32] Y. Ninomiya, W. Bentz, and I. C. Cloët, Phys. Rev. C **91**, 025202 (2015).
[33] J. Badier *et al.* (NA3 Collaboration), Z. Phys. C **18**, 281 (1983).
[34] J. S. Conway *et al.*, Phys. Rev. D **39**, 92 (1989).
[35] S. D. Drell and T. M. Yan, Phys. Rev. Lett. **24**, 181 (1970).
[36] G. B. West, Phys. Rev. Lett. **24**, 1206 (1970).
[37] J. S. Schwinger, Phys. Rev. **82**, 664 (1951).
[38] D. Ebert, T. Feldmann, and H. Reinhardt, Phys. Lett. B **388**, 154 (1996).
[39] G. Hellstern, R. Alkofer, and H. Reinhardt, Nucl. Phys. A **625**, 697 (1997).
[40] W. Bentz and A. W. Thomas, Nucl. Phys. A **696**, 138 (2001).
[41] S. P. Klevansky, Rev. Mod. Phys. **64**, 649 (1992).
[42] U. Vogl and W. Weise, Prog. Part. Nucl. Phys. **27**, 195 (1991).
[43] U. Vogl, M. F. M. Lutz, S. Klimt, and W. Weise, Nucl. Phys. A **516**, 469 (1990).
[44] T. Hatsuda and T. Kunihiro, Phys. Rep. **247**, 221 (1994).
[45] M. Buballa, Phys. Rep. **407**, 205 (2005).
[46] N. Ishii, W. Bentz, and K. Yazaki, Nucl. Phys. A **587**, 617 (1995).
[47] H. Mineo, W. Bentz, N. Ishii, A. W. Thomas, and K. Yazaki, Nucl. Phys. A **735**, 482 (2004).
[48] I. C. Cloët, W. Bentz, and A. W. Thomas, Phys. Rev. Lett. **95**, 052302 (2005).
[49] I. C. Cloët, W. Bentz, and A. W. Thomas, Phys. Lett. B **642**, 210 (2006).
[50] I. C. Cloët, W. Bentz, and A. W. Thomas, Phys. Lett. B **659**, 214 (2008).
[51] I. C. Cloët, W. Bentz, and A. W. Thomas, Phys. Rev. C **90**, 045202 (2014).
[52] M. E. Carrillo-Serrano, I. C. Cloët, and A. W. Thomas, Phys. Rev. C **90**, 064316 (2014).
[53] T. Klähn, R. Lastowiecki, and D. B. Blaschke, Phys. Rev. D **88**, 085001 (2013).
[54] S. Lawley, W. Bentz, and A. W. Thomas, Nucl. Phys. Proc. Suppl. **141**, 29 (2005).
[55] M. Baldo, G. F. Burgio, P. Castorina, S. Plumari, and D. Zappala, Phys. Rev. C **75**, 035804 (2007).
[56] T. Ito, W. Bentz, I. C. Cloët, A. W. Thomas, and K. Yazaki, Phys. Rev. D **80**, 074008 (2009).
[57] H. H. Matevosyan, A. W. Thomas, and W. Bentz, Phys. Rev. D **88**, 094022 (2013).
[58] H. H. Matevosyan, W. Bentz, I. C. Cloët, and A. W. Thomas, Phys. Rev. D **85**, 014021 (2012).
[59] T. Horikawa and W. Bentz, Nucl. Phys. A **762**, 102 (2005).
[60] C. Weiss, A. Buck, R. Alkofer, and H. Reinhardt, Phys. Lett. B **312**, 6 (1993).
[61] G. Ripka, Czech. J. Phys. **46**, 721 (1996).
[62] W. Broniowski, G. Ripka, E. Nikolov, and K. Goeke, Z. Phys. A **354**, 421 (1996).
[63] J. Bijnens, Phys. Rep. **265**, 369 (1996).
[64] D. Ebert, T. Feldmann, R. Friedrich, and H. Reinhardt, Nucl. Phys. B **434**, 619 (1995).
[65] J. Beringer *et al.* (Particle Data Group), Phys. Rev. D **86**, 010001 (2012).
[66] S. Durr *et al.*, Phys. Lett. B **701**, 265 (2011).
[67] S. R. Amendolia *et al.*, Phys. Lett. B **146**, 116 (1984).
[68] S. R. Amendolia *et al.* (NA7 Collaboration), Nucl. Phys. B **277**, 168 (1986).
[69] T. Horn *et al.* [Jefferson Lab F(pi)-2 Collaboration], Phys. Rev. Lett. **97**, 192001 (2006).
[70] V. Tadevosyan *et al.* [Jefferson Lab F(pi) Collaboration], Phys. Rev. C **75**, 055205 (2007).
[71] G. M. Huber *et al.* (Jefferson Lab Collaboration), Phys. Rev. C **78**, 045203 (2008).
[72] H. P. Blok *et al.* (Jefferson Lab Collaboration), Phys. Rev. C **78**, 045202 (2008).
[73] H. J. Munczek, Phys. Rev. D **52**, 4736 (1995).
[74] S. R. Amendolia *et al.*, Phys. Lett. B **178**, 435 (1986).
[75] T. Horn and C. D. Roberts, J. Phys. G: Nucl. Part. Phys. **G43**, 073001 (2016).
[76] K. A. Olive *et al.* (Particle Data Group), Chin. Phys. C **38**, 090001 (2014).

[77] G. P. Lepage and S. J. Brodsky, Phys. Lett. B **87**, 359 (1979).
[78] V. N. Gribov and L. N. Lipatov, Sov. J. Nucl. Phys. **15**, 675 (1972) [Yad. Fiz. **15**, 1218 (1972)].
[79] G. Altarelli and G. Parisi, Nucl. Phys. B **126**, 298 (1977).
[80] Y. L. Dokshitzer, Sov. Phys. JETP **46**, 641 (1977) [Zh. Eksp. Teor. Fiz. **73**, 1216 (1977)].
[81] M. Miyama and S. Kumano, Comput. Phys. Commun. **94**, 185 (1996).
[82] M. Aicher, A. Schafer, and W. Vogelsang, Phys. Rev. Lett. **105**, 252003 (2010).
[83] J. Badier *et al.* (Saclay-CERN-College de France-Ecole Poly-Orsay Collaboration), Phys. Lett. B **93**, 354 (1980).
[84] P. Maris and C. D. Roberts, Int. J. Mod. Phys. E **12**, 297 (2003).
[85] G. R. Farrar and D. R. Jackson, Phys. Rev. Lett. **43**, 246 (1979).